SCIENCE CHINA
Chemistry

• ARTICLES •

December 2013 Vol.56 No.12: 1775–1782
doi: 10.1007/s11426-013-4948-z

Heterogeneous degradation of toxic organic pollutants by hydrophobic copper Schiff-base complex under visible irradiation

SONG Quan[1], JIA ManKe[1,2], MA WanHong[1,2], FANG YanFen[1,2] & HUANG YingPing[1,2*]

[1]*Engineering Research Center of Eco-environment in Three Gorges Reservoir Region, Ministry of Education, China Three Gorges University, Yichang 443002, China*

[2]*Collaborative Innovation Center for Geo-Hazards and Eco-Environment in Three Gorges Area, Hubei Province, Yichang 443002, China*

Received April 26, 2013; accepted June 6, 2013; published online September 25, 2013

A hydrophobic complex of Cu^{2+}[bis-salicylic aldehyde-*o*-phenylenediamine], Cu-SPA, was prepared and used as a heterogeneous photocatalyst to degrade organic pollutants in water under visible irradiation ($\lambda \geqslant 420$ nm) at neutral pH. The structure of complex was characterized by using nuclear magnetic resonance (NMR), elemental analysis, IR and UV-vis spectrometries. Degradation of Rhodamine B (RhB), Sulforhodamine B (SRB) and Benzoic acid (BA) in water were used as model reactions to evaluate the photocatalytic activities of Cu-SPA. The results indicated that RhB and SRB were easily adsorbed on the hydrophobic surface of Cu-SPA from aqueous solution (the maximum adsorption amount: Q_{max} = 11.09 and 8.05 μmol/g, respectively). Under visible irradiation, RhB and SRB were decolorized completely after 210 and 240 min, respectively, and BA was removed completely after 5 h. The efficiency of H_2O_2 was > 95%, in contrast to that of the reaction without catalyst or light (< 20%). In water soluble medium, the hydrophobic Cu-SPA can be used more than 6 cycles. ESR results and the behavior of cyclic voltammetry showed that, in the reaction process, Cu^{2+}-SPA was reduced to intermediate state Cu^{+}-SPA firstly, which was extremely unstable and reacted rapidly with H_2O_2, leading to high reactive oxygen species (·OH radical) to degrade the substrate.

hydrophobic, copper Schiff-base, photocatalysis, toxic organic pollutant

1 Introduction

In recent years, advanced oxidation processes (AOPs) represent a powerful mean for the abatement of refractory and toxic pollutants in wastewater [1–4]. The Fenton and photo-Fenton processes are known as effective AOPs methods to remove organic pollutants from wastewater [5, 6]. In these processes, hydrogen peroxide is activated by dissolved iron or UV irradiation to produce high reactive species, mainly ·OH, which oxidize the organic compounds [7–10]. However, the main drawbacks in Fenton and photo-Fenton processes, such as the necessity of working at low pH (pH ⩽ 3), the expensive UV light source and the difficulty of recycling restrict its practical application [11, 12]. Enzyme-based treatment is sufficient in transforming toxic compounds to less harmful products, which had minimal impact on ecosystem [13–16]. Peroxidases and Laccases are oxidative enzymes which do not need any other cellular components to work. They have broad substrate specificity and are able to transform a wide range of toxic compounds [14]. However, the cost of these biocatalysts is still too high to implement commercially attractive enzyme-based treatments in industrial applications.

Exploring adaptive mimic-enzyme systems combined with clean oxidants such as O_2 or H_2O_2 to replace the traditional biocatalysts, which are too expensive to application, has become one of the most attractive targets in organic syntheses [17–20]. Existing research indicates that, some of the metal-organic complex, such as metal-porphyrin and

*Corresponding author (email: huangyp@ctgu.edu.cn)

metal-phthalocyanine, have strong absorption in the visible light region and can activate O_2 or H_2O_2 to oxidize or degrade toxic organic pollutants [21–24], being similar to peroxidases [25, 26]. Furthermore, the stability and catalytic activity of catalyst can be improved effectively through the optimization of ligand, changing the bionic compound micro environment and loading to form heterogeneous catalyst [27]. The metal Schiff-base complex has attracted much attention also, due to the peculiar electronic characteristics, stable structure, and adjusting the electronic and space effect of complex accurately and easily by changing the ligand or metal ion [28–30]. The copper Schiff-base can act as catalyst in lots of oxidation reactions because it can imitate biological enzyme [31, 32]. At present, many copper Schiff- base complexes have been reported about the selective catalytic oxidation of different group mainly in homogeneous reaction [33–35], but few research pays attention to the heterogeneous photocatalytic performance in water treatment of toxic organic pollutants under visible light [36]. The advantage of heterogeneous catalyst stems from easy separation from the reaction solution. More interesting, it can form hydrophobic micro environmental mimic enzyme catalytic properties, and avoid the axial aggregation and degradation itself.

In this study, we synthesized the hydrophobic copper Schiff-base complex and used it as heterogeneous photocatalyst to degrade organic pollutants, mimicking the active centre of laccases [15], under visible irradiation ($\lambda \geqslant 420$ nm) at neutral pH. The structure of the catalyst was characterized by using nuclear magnetic resonance (NMR), elemental analysis, IR spectrum and UV-vis absorption spectrum. The photocatalytic degradation of Rhodamine B (RhB), Sulforhodamine B (SRB) and Benzoic acid (BA) were used as probe reactions to evaluate the photocatalytic activities of Cu-SPA. The mechanism of photocatalytic oxidation was discussed according to the oxidation species during the degradation process and the behavior of cyclic voltammetry.

2 Experimental

2.1 Materials

Salicylide, *o*-phenylenediamine, cupric nitrate ($Cu(NO_3)_2 \cdot 3H_2O$), and anhydrous ethanol were of A.R. grade, as well as H_2O_2 solution (30%) were obtained from the Tianli Chemical Factory (Tianjin, China). RhB, SRB and BA were purchased from Beijing Ouhe Chemical Factory (China), other chemicals were of reagent grade and used without further purification. Deionized and doubly distilled water was used throughout the investigation.

2.2 Synthesis

2.2.1 Synthesis of SPA ligand

The Schiff base (bis-salicylic aldehyde-*o*-phenylenediamine, SPA) was prepared as previously described [36]. The yield of SPA obtained in this manner was about 85%. The purity and structure of the prepared SPA were checked by the melting point constancy, elemental analysis and ^{1}H NMR, respectively, and the results were: m.p., 163.7–164.5 °C; element composition (%, calculated value), C 75.83 (75.93), H 5.00 (5.10), N 8.83 (8.86); ^{1}H NMR (400 MHz, CD_3COCD_3), δ 6.938–6.981 (m, 4H, H_a, H_c), 7.390–7.457 (m, 6H, H_b, H_f, H_g), 7.572–7.595 (dd, 2H, H_d), 8.878 (s, 2H, H_e), 13.009 (s, 2H, OH).

2.2.2 Synthesis of Cu-SPA complex

The Cu-SPA complex was obtained by mixing $Cu(NO_3)_2 \cdot 3H_2O$ and SPA (1:1, molar ration) in anhydrous ethanol solvent. The green solution thus formed turned to a brownish precipitate, and the mixture was heated under reflux at 80 °C for 4 h and then cooled. The product was then filtered off, washed thoroughly with anhydrous ethanol and dried in an open air. The yield of Cu-SPA obtained in this manner was 67.5%. The elemental analysis found (%, calculated value): C 54.47 (54.61), H 3.23 (3.18), and N 9.43 (9.55).

2.3 Instrumental analyses

UV-vis and IR spectra were acquired at room temperature using Lambda 25 spectrophotometer (PE, America) and NEXUS670 Infrared spectrometer (Thermo Electron, America), respectively. The NMR and elemental analyses were performed using AVANCE^{TM}III400 superconducting Fourier nuclear magnetic resonance spectrometer (Bruker, Switzerland) and VARIOEL III Element analyzer (Eementar Analysensysteme, Germany). The copper content was determined by AAS-240FS+GTA120 atomic absorption spectrophotometer (Varian, America).

2.4 Catalytic activity under visible light

The light source was a 500 W halogen lamp positioned in a XPA series photochemical reaction instrument. A cut off filter was placed outside the Pyrex jacket to eliminate any

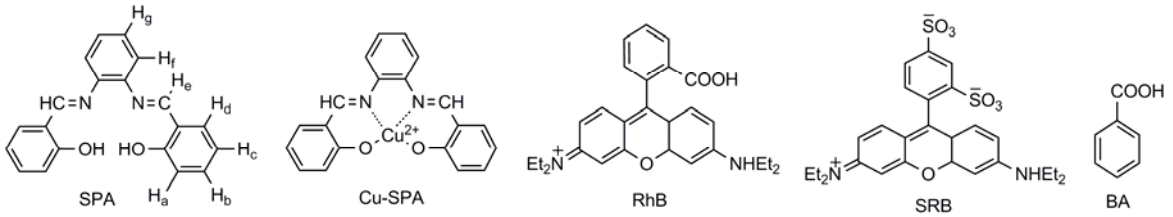

Figure 1 Molecular structures of SPA, Cu-SPA, RhB, SRB and BA.

radiation at wavelength below 420 nm to ensure illumination by visible light only. 40 mL RhB or SRB containing 8 mg Cu-SPA, contrasting with equimolar Cu^{2+}, and appropriate H_2O_2 were put into a cylindrical glass bottle and the pH was adjusted. The above solutions were placed in dark for 3 h to achieve the adsorption and desorption-balance and then sampled in different time intervals with Ep tube in the visible light ($\lambda \geqslant 420$ nm). Samples were centrifuged and analyzed with UV-vis and FTIR spectrophotometers.

The method was also applied to BA, but the samples were determined by HPLC. And the mobile phase was methanol and 0.02 mol/L ammonium acetate aqueous solution, and the ratio was 35:65. The flow rate was 0.50 mL/min, and the detection wavelength was 215 nm.

2.5 Determination of active radicals

The oxidative active radicals produced in the process of reaction were measured with ESR method [38]. In order to reduce the experimental errors, the same quartz capillary was used in the whole process. DMPO was put in the reacting systems to capture the ·OH produced. Hydrogen peroxide was analyzed by a spectrophotometric method using dipotassium titanium oxide and oxysulfate (DIN38 402 H15 method), which forms a yellow complex with H_2O_2 (maximum absorption at 400 nm).

2.6 The cyclic voltammetry (CV) measurement of SPA and Cu-SPA

Cyclic voltammetry was performed on a CH instrument electrochemical station model CHI660D (Chenhua, China) with a glassy carbon working electrode (diameter = 5 mm), a platinum-wire counter electrode and a saturated calomel electrode (SCE). Potassium ferricyanide was used as internal reference. Controlled-potential electrolysis was performed on a reticulated vitreous carbon working electrode, a platinum-wire counter electrode and a SCE reference electrode in an anhydrous ethanol solution containing the supporting electrolytes (0.5 mol/L $NaClO_4 \cdot H_2O$ in anhydrous ethanol) and appropriate complex or ligand.

3 Results and discussion

3.1 Characterization

IR analyses of the ligand and complex were presented in Table 1. For the SPA, two absorption bands at 3500–3420 and 1420–1380 cm^{-1} were assigned to ν(O–H) stretching and δ(O–H) rocking, which indicated the presence of the phenolic hydroxyl. These bands disappeared in the complex, as a result of proton substitution by Cu^{2+} coordination to oxygen. And several IR absorption bands at 1650–1450 cm^{-1} can be attributed to the ν(C=C) and ν(C=N) stretchings [37]. The ν(C=N) stretching of Cu-SPA appeared at 1609 cm^{-1}, which occurred red shift comparing with the ligand and indicated that N atom participated in coordination. For the complex, a weak band observed at 630–510 cm^{-1} can be attributed to the ν(Cu–N) and ν(Cu–O), which further confirmed the stability of the Cu-SPA and its coordination mode.

The UV-vis spectra of both SPA and complex were measured in methanol (Figure 2). For the ligand, two absorption bands were observed at the range of 240–450 nm, which were assigned to π-π* transition in the conjugation of C=N with benzene ring and the intraligand n-π* transition. The spectrum of the Cu-SPA complex exhibited an absorption band at 420 nm that was assigned to d-d transition [32]. These absorptions of π→π* and n→π* transitions also present in the spectrum of the copper complex but they shifted. This shift of the complex originated from the N atom in C=N, which has lone pair electrons participating in coordination while the H atom of –OH was replaced by Cu^{2+}. It changed the conjugation system and electronic properties of molecular, and was conducive to visible catalytic oxidation reaction.

The UV-vis DRS spectrum of Cu-SPA (Figure 3) showed that Cu-SPA has a strong absorption in the visible region (400–700 nm), which evinced the visible catalytic performance of Cu-SPA.

3.2 Adsorption of organic compounds on Cu-SPA

The adsorption behavior on the catalyst surface is an important factor in photocatalytic reaction process. The efficiency of degradation of pollutants can be obviously enhanced by the adsorption of organic pollutants onto the interface of catalyst. In this study, the adsorption capacity was calculated according to the adsorption equilibrium equation of Langmuir model as follows:

$$Q_{eq}^{-1} = (Q_{max}KC_{eq})^{-1} + Q_{max}^{-1}$$

where Q_{eq} is the equilibrium adsorption capacity, Q_{max} is the maximum adsorption capacity, K is the adsorption equilib-

Table 1 IR data of ligand and complex (cm^{-1})

	ν (ArO–H) [a)]	ν (C=N)	ν (–C=C–)	δ(ArO–H)	ν (Ar–O)	ν (Cu–O)	ν (Cu–N)
SPA	3446	1616	1586、1562、1481	1403	1193	–	–
Cu-SPA	–	1609	1580、1530、1462	–	1189	619	538

a) Ar = benzene ring.

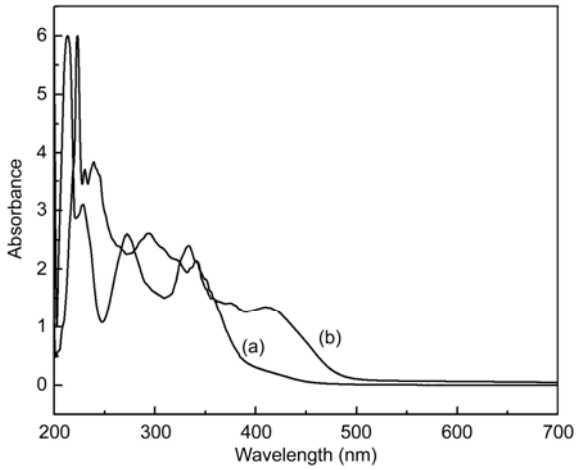

Figure 2 UV-vis absorption spectra of SPA (a) and Cu-SPA (b).

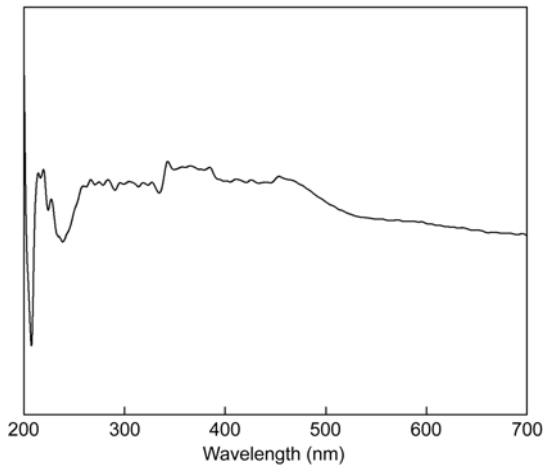

Figure 3 UV-vis DRS spectrum of Cu-SPA.

rium constant, and C_{eq} is the adsorption equilibrium concentration. Table 2 presented the adsorption parameters of RhB and SRB with Cu-SPA at pH 7.0. The Q_{max} of RhB and SRB on Cu-SPA was 8.53 and 11.09 μmol/g, respectively. The surface area is an important key to the adsorption activities of the catalyst. The specific surface area of Cu-SPA is 4.71 m^2/g, which was estimated from the low-temperature nitrogen adsorption and desorption isothermal curves. It may be beneficial to increase the adsorption sites on the surface of Cu-SPA, which is the important factor to the adsorption capacity. These results indicated that Cu-SPA had good adsorption properties for both RhB and SRB, which was attributed to large specific surface area of Cu-SPA, and the strong hydrophobic interaction between substrates and Cu-SPA particles.

3.3 Heterogeneous photocatalytic degradation of organic compounds using Cu-SPA

The photocatalytic activities of Cu-SPA were tested by degradation of RhB and SRB. Figure 4 showed the degradation kinetic curves under different conditions. According to linear fitting of degradation of RhB, the values of kinetic constant were $k_a = 0$, $k_b = 8.651 \times 10^{-4}$ min^{-1}, $k_c = 9.691 \times 10^{-4}$ min^{-1}, $k_d = 1.404 \times 10^{-2}$ min^{-1}. It indicated that Cu-SPA could activate H_2O_2 and degrade RhB effectively under visible irradiation. The UV-vis absorption spectra of RhB in Vis/Cu-SPA/H_2O_2/RhB system were shown in the inset of Figure 4(A). The maximum absorption peak of RhB at 553 nm was reduced continuously in the reaction process, which demonstrated that chromogenic conjugated ring of RhB was destructed. RhB was completely decolorized after 210 min. In order to affirm the activities of Cu-SPA in de-

Table 2 Adsorption parameters of RhB or SRB on Cu-SPA

Dyes	Q_{max} (μmol/g)	K	R^2
RhB	8.53	0.036	0.999
SRB	11.09	0.523	0.996

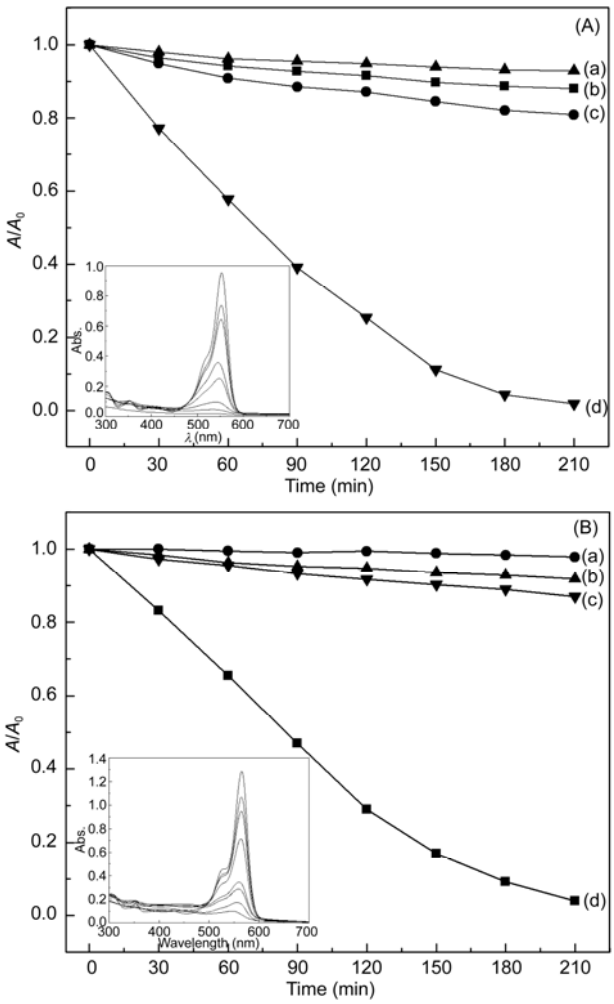

Figure 4 Photodegradations of RhB (A) and SRB (B) under different conditions. (a) Vis/Cu^{2+}/H_2O_2; (b) Dark/Cu-SPA/H_2O_2; (c) Vis/H_2O_2; (d) Vis/Cu-SPA/H_2O_2. [Cu-SPA] = 0.20 g/L, [H_2O_2] = 1.50×10^{-3} mol/L, pH 7.0, [RhB/SRB] = 1.25×10^{-5} mol/L.

grading dye molecules, SRB was also regarded as probe to discuss the photocatalytic activities, and the kinetic curves were shown in Figure 4(B). It also showed good photocatalytic activity of Cu-SPA on degrading SRB, which was decolorized completely after 240 min in Vis/Cu-SPA/H_2O_2/SRB system. The UV-vis absorption spectra of SRB were shown in the inset of Figure 4(B). Results of the study showed that, under visible light irradiation, H_2O_2 was activated effectively by Cu-SPA to degrade toxic and organic contaminants.

It is well known that the photocatalytic oxidation of toxic colorless small molecules can be used to evaluate the photocatalytic activities of catalyst. In order to further examine the role of Cu-SPA in the photocatalytic reaction, BA, a stable organic substance that does not absorb visible light, was selected as a target compound. The experiments were done at pH 6.8 in the presence of Cu-SPA and H_2O_2. Degradation curves were displayed in Figure 5 which were similar to those obtained for RhB and SRB. Control experiments showed that, under otherwise identical conditions, there was only slight degradation of BA observed (29.67% after 5 h) in the presence of H_2O_2 alone (Figure 5(b)). In dark, almost no degradation occurred (2.16% after 5 h) containing both Cu-SPA and H_2O_2 (Figure 5(b)). In the presence of Cu-SPA and H_2O_2 (Figure 5(c)), 98.61% of BA was degraded after 5 h of visible irradiation. The results indicated that the photocatalytic system under investigation was efficient at degrading small stable organic molecules. It showed that Cu-SPA can act as an effective catalyst and activate H_2O_2 to degrade toxic organic pollutants, which did not attribute to photosensitization process.

3.4 Effect of pH

To evaluate the effect of pH, the degradation of RhB using Cu-SPA and H_2O_2 was carried out under visible light irradiation at different pH values. It was found that the degradation rate of RhB increased firstly and then decreased with pH values from 3.0 to 11.0 (Figure 6). The results indicated that Cu-SPA was similar to the natural enzyme and had higher activity at neutral pH. Furthermore, the photocatalyst exhibited catalytic activity at a wide pH range, which was unlike traditional (Photo) Fenton system (only in the medium of pH < 3.0). Under visible light irradiation, Cu-SPA overcame the limit of pH and broadened the range of pH in the photocatalytic system.

3.5 Infrared analysis of RhB degradation

The degradation products of Vis/Cu-SPA/H_2O_2/RhB system in different time were analyzed by infrared spectrophotometry (Figure 7). For the original RhB, the absorption peaks

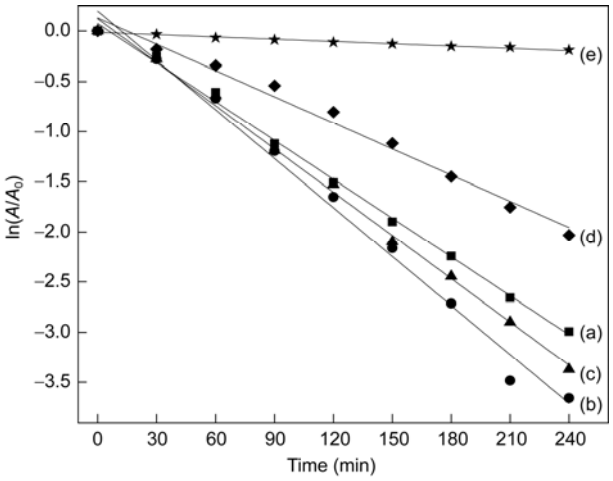

Figure 6 Effect of pH on the degradation of RhB. (a) pH 3.0; (b) pH 5.0; (c) pH 7.0; (d) pH 9.0; (e) pH 11.0. [RhB] = 1.25×10^{-5} mol/L, [Cu-SPA] = 0.20 g/L, [H_2O_2] = 1.5×10^{-3} mol/L.

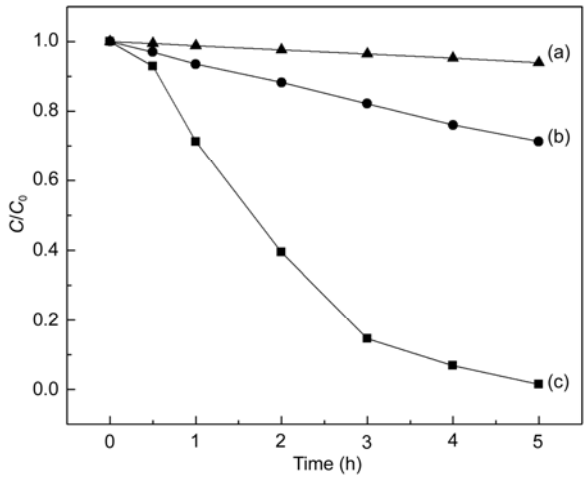

Figure 5 Kinetic curves for photocatalytic degradation of BA. (a) Dark/Cu-SPA/H_2O_2; (b) Vis /H_2O_2; (c) Vis/Cu-SPA/H_2O_2. [BA] = 5×10^{-4} mol/L, [Cu-SPA] = 0.20 g/L, [H_2O_2] = 1.5×10^{-3} mol/L, pH 6.8.

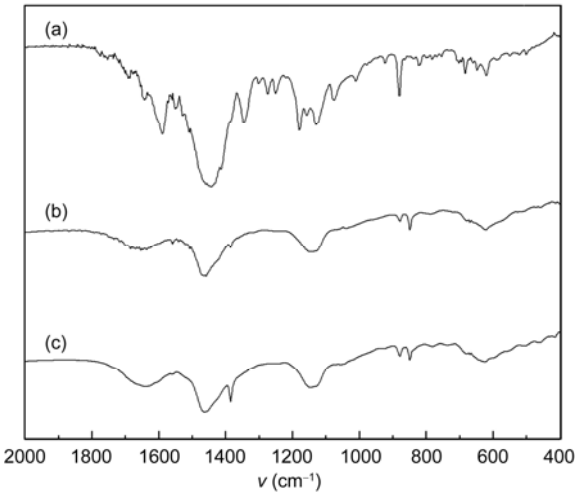

Figure 7 IR spectra of intermediates in the degradation of RhB. (a) 0 h; (b) 8 h; (c) 16 h. [RhB] = 1.25×10^{-5} mol/L, [Cu-SPA] = 0.20 g/L, [H_2O_2] = 1.5×10^{-3} mol/L, pH 7.0.

at 1589, 1340 and 1180 cm^{-1} were attributed to the vibration of benzene ring, the ν(C–CH_3) stretching and ν(Ar–N) stretching, respectively. The absorption peaks at 1440 and 1079 cm^{-1} could be attributed to the ν(–C=C–) stretching of benzene ring and ν(–C–O–C–) stretching, respectively. For the degradation products at 8 or 16 h, the characteristic peaks at 1589, 1340, 1180, 1079, and 923 cm^{-1} disappeared. Meanwhile, new characteristic peaks, such as 1630 cm^{-1} attributed to $\delta(NH_2)$ bending, 1380 cm^{-1} attributed to ν(COOH) stretching and 1120 cm^{-1} attributed to ν(C–N) stretching appeared. It indicated that the Ar–N and –C–O–C– in RhB molecule were broken and transformed into primary amines and carboxylic acids. The results evinced RhB was destroyed gradually in degradation process and some new substances produced.

3.6 Determination of H_2O_2 in RhB degradation process

In order to assess the utilization of H_2O_2 in reaction by Cu-SPA, experiments on RhB degradation in dark and under visible light at pH 7.0 were carried out with Cu-SPA. The concentration of H_2O_2 in degradation process was measured by titanium salt spectrophotometry (Figure 8). It showed that the decomposition of H_2O_2 after 12 h in Dark/Cu-SPA/H_2O_2/RhB system (Figure 8(b)) and Vis/H_2O_2/RhB system (Figure 8(a)) were 16.3% and 19.8%, respectively, which indicated that H_2O_2 was not utilized significantly. But H_2O_2 was decomposed rapidly (95.1%) in Vis/Cu-SPA/H_2O_2 system (Figure 8(c)), and the RhB was degraded rapidly (Figure 8(d)). The experiments indicated that Cu-SPA can activate H_2O_2 efficiently under visible light.

3.7 Stability of Cu-SPA

The performance of the catalyst in recycling experiments is significant for its application in environmental technology. Thus, cycle experiments of Vis/CuSPA/ H_2O_2 system degrading RhB were carried out with pH 7.0, as shown in Figure 9. The content of copper ion liberated from Cu-SPA was determined by atomic absorption spectrometry (AAS). After the RhB was degraded completely, the catalyst was seperated from the bulk solution, and then RhB and H_2O_2 were rejoined. After 5 consecutive cycles, the liberated copper ion was 14.75% (dot line, Figure 9) and the catalyst still showed good stability and reusability in the aqueous system.

3.8 Possible mechanism for the photocatalytic degradation of RhB

Free Cu^{2+}/H_2O_2 exhibits high oxidative activity in degradation of organic pollutants, stemming from its ability to initiate redox cycling, in turn generating high reactive oxygen species (ROS) via the Harber-Weiss reaction [30]:

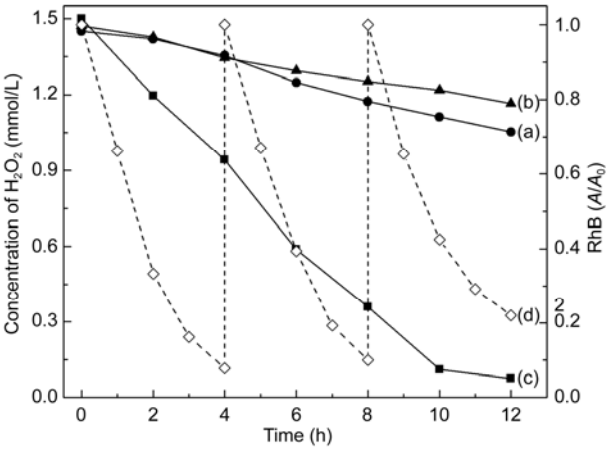

Figure 8 Measurement of H_2O_2 in the degradation process. (a) Vis/H_2O_2/RhB; (b) Dark/Cu-SPA/H_2O_2/RhB; (c) Vis/Cu-SPA/H_2O_2/RhB; (d) concentration of RhB. [RhB] = 1.25×10^{-5} mol/L, [Cu-SPA] = 0.20 g/L, [H_2O_2] = 1.5×10^{-3} mol/L, pH 7.0.

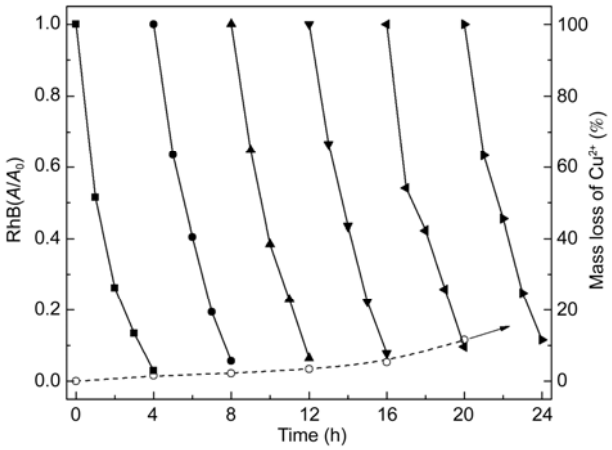

Figure 9 Catalyst recycling in repetitive degradation of RhB (solid line) and the content of copper ion (dot line). [RhB] = 1.25×10^{-5} mol/L, [Cu-SPA] = 0.20 g/L, [H_2O_2] = 1.5×10^{-3} mol/L, pH 7.0.

$$Cu^{2+} + H_2O_2 \rightarrow Cu^{+}\cdot O_2H + H^{+} \quad (1)$$

$$Cu^{+}\cdot O_2H + H_2O_2 \rightarrow Cu^{+} + O_2 + \cdot OH + H_2O \quad (2)$$

$$H^{+} + Cu^{+} + H_2O_2 \rightarrow Cu^{2+} + \cdot OH + H_2O \quad (3)$$

Unlike free Cu^{2+} in Fenton system, the central Cu^{2+} in Cu-SPA was coordinated with the schiff base ligand. Therefore, the Cu^{2+} could not be readily reduced to Cu^{+} by H_2O_2, which was a key intermediate in Cu^{2+} catalytic Fenton reaction. In our previous work, we found that hydroxyl radicals (·OH) were the main ROS during the degradation of RhB with H_2O_2 as oxidant and iron (III) Schiff base as photocatalyst, which involved two mechanisms, namely electron transfer of center metal iron similar to Fenton reaction and the oxidative performance of high-valence iron-oxo species [36].

In order to detect the possibility of generating ·OH during the degradation process, electron spin resonance (ESR) method was used, and DMPO was employed as the spin-trapping reagent. The results were shown in Figure 10. It was clearly observed that the characteristic 1:2:2:1 quartet ESR signal, which was typically attributed to the ESR spectrum of the DMPO–·OH adduct, generated after introducing visible light [38]. As a control experiment, no ESR signal was detected in dark. It clearly indicated ·OH generated in the presence of Cu-SPA and H_2O_2, and the mechanism of degradation involved the ·OH oxidation mechanism.

The photoexcitation of Cu-SPA and the subsequent formation of ·OH under visible light irradiation can be described as follows. Cu^{2+}-SPA is excited by light irradiation and undergoes MLCT to produce Cu^{+}-SPA, which has high reducibility and electronegativity. Cu^{+}-SPA then interacts with H_2O_2 to generate ·OH, which subsequently oxidizes the substrate by the following mechanism:

$$Cu^{2+}\text{-SPA} \rightarrow Cu^{+}\text{-SPA}^* \quad (4)$$

$$Cu^{+}\text{-SPA}^* + H_2O_2 \rightarrow Cu^{2+}\text{-SPA} + {}^{\cdot}OH + {}^{-}OH \quad (5)$$

$$^{\cdot}OH + \text{subs} \rightarrow \text{oxidation products} \quad (6)$$

As described above, the central copper could transfer the electrons to H_2O_2 through a key intermediate, Cu^{+}-SPA species. And the transformation was probably promoted by the Schiff base ligand. The above fact was demonstrated by the cyclic voltammetry (CV) of Cu-SPA. The cyclic voltammetry of Cu–SPA was carried out in methanol solution at room temperature at the potential from 0.2 to 1.2 V (versus SCE, Figure 11). The cyclic voltammogram exhibited three reduction peaks at 0.54 (I), 0.91 (II) and 1.56 V (III). Peak I and II were ascribed to the electron transfer from predominantly ligand-centered orbital [35] and the reduction of Cu^{2+}-SPA to Cu^{+}-SPA, respectively. Peak III corresponded to reduction of SPA, which shifted about 0.17 V due to its coordination with Cu^{2+} comparing with the SPA (reduction peak at 1.39 V). These can be concluded that, in the photocatalytic reaction, Cu^{2+}-SPA was reduced to intermediate state Cu^{+}-SPA firstly, which was similar to activity center of Laccase, then extremely unstable Cu^{+}-SPA reacted rapidly with H_2O_2.

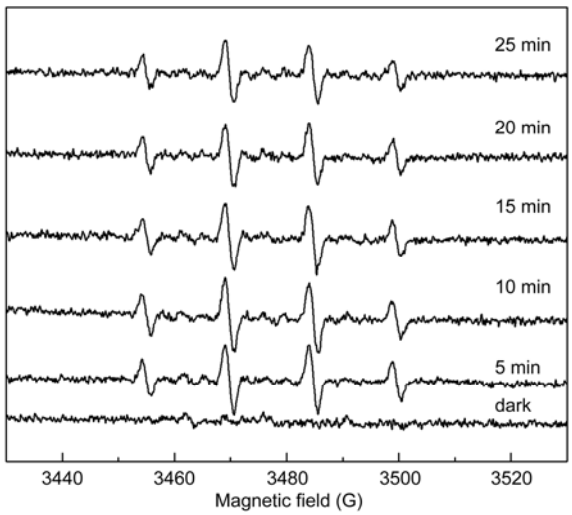

Figure 10 ESR signals of the DMPO–OH adducts in water. [DMPO] = 0.04 mol/L, [Cu-SPA] = 0.20 g/L, [H_2O_2] = 1.5×10^{-3} mol/L.

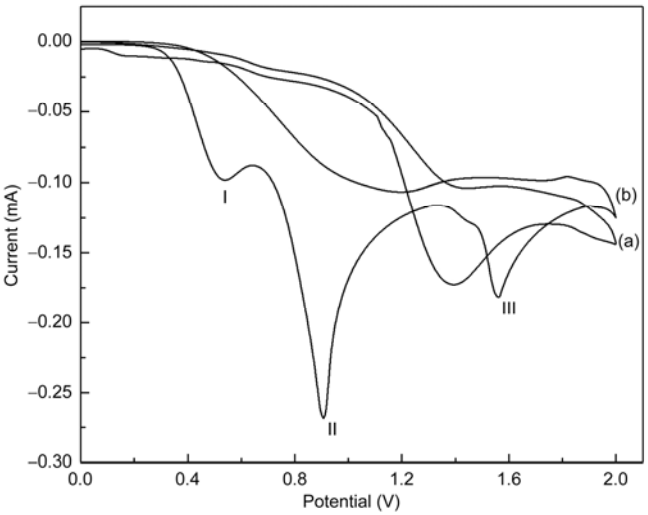

Figure 11 Cyclic voltammogram curves of SPA (a) and Cu-SPA (b) in methanol on glassy carbon electrode. [Cu-SPA] = 0.02 g/L, [SPA] = 0.02 g/L, [$NaClO_4$] (supporting electrolyte) = 0.1 mol/L, V = 20 mV/s

4 Conclusions

The hydrophobic complex Cu^{II}(bis-salicylic aldehyde-*o*-phenylenediamine), Cu-SPA, had been successfully prepared by simple chemical method and characterized by using NMR, elemental analysis, IR and UV-vis spectrometries. Results of the present study clearly implied that Cu-SPA can be used as heterogeneous catalyst to degrade toxic organic pollutants in aqueous system. Under visible light irradiation, Cu-SPA could efficiently activate H_2O_2 to produce ·OH, which degraded organic pollutants effectively due to its highly oxidizing activity. Heterogeneous catalytic system was formed via the hydrophobic properties of catalyst, which had good stability and reusability. Cu-SPA showed good catalytic activity in a wide range of pH (< 11) and expanded its scope of application.

This work was supported by the National Natural Science Foundation of China (21207079, 21307073, 21177072, 21377067).

1 Kubacka A, Fernández-García M, Colón G. Advanced nanoarchitectures for solar photocatalytic applications. *Chem Rev*, 2012, 112: 1555–1614

2 O'shea KE, Dionysiou DD. Advanced oxidation processes for water treatment. *J Phys Chem Lett*, 2012, 3: 2112–2113

3 Quici N, Litter MI. Photochemical advanced oxidation processes for water and wastewater treatment. *Recent Pat Eng*, 2010, 4: 217–241
4 Mira P, Jelena R, Damia B. Advanced oxidation processes (AOPs) applied for wastewater and drinking water treatment. Elimination of pharmaceuticals. *Holistic Ap Environ*, 2011, 2: 63–74
5 Malato S, Fernández-Ibáñez P, Maldonado MI, Blanco J, Gernjak W. Decontamination and disinfection of water by solar photocatalysis: Recent overview and trends. *Catal Today*, 2009, 147: 1–59
6 Lamsal R, Walsh ME, Gagnon GA. Comparison of advanced oxidation processes for the removal of natural organic matter. *Water Res*, 2011, 45: 3263–3269
7 Elias RJ, Waterhouse AL. Controlling the fenton reaction in wine. *J Agric Food Chem*, 2010, 58: 1699–1707
8 Ahmed B, Limem E, Abdel-Wahab A, Nasr B. Photo-fenton treatment of actual agro-industrial wastewaters. *Ind Eng Chem Res*, 2011, 50: 6673–6680
9 Chen LW, Ma J, Li XC, Zhang J, Fang JY, Guan YH, Xie PC. Strong enhancement on Fenton oxidation by addition of hydroxylamine to accelerate the ferric and ferrous iron cycles. *Environ Sci Technol*, 2011, 45: 3925–3930
10 Zazo JA, Pliego G, Blasco S, Casas JA, Rodriguez L. Intensification of the fenton process by increasing the temperature. *Ind Eng Chem Res*, 2011, 50: 866–870
11 Navalon S, Alvaro M, Garcia H. Heterogeneous Fenton catalysts based on clays, silicas and zeolites. *Appl Catal B: Environ*, 2010, 99: 1–26
12 Gonzalez-Olmos R, Martin MJ, Georgi A, Kopinke FD, Oller I, Malato S. Fe-zeolites as heterogeneous catalysts in solar Fenton-like reactions at neutral pH. *Appl Catal B: Environ*, 2012, 125: 51–58
13 Burton SG. Oxidizing enzymes as biocatalysts. *Trends Biotechnol*, 2003, 21: 543–549
14 Torres E, Bustos-Jaimes I, Le Borgne SL. Potential use of oxidative enzymes for the detoxification of organic pollutants. *Appl Catal B: Environ*, 2003, 46: 1–15
15 Riva S. Laccases: Blue enzymes for green chemistry. *Trends Biotechnol*, 2006, 24: 219–226
16 Karigar CS, Rao SS. Role of microbial enzymes in the bioremediation of pollutants: A review. *Enzyme Res*, 2011, 2011: 1–11
17 Li J, Ma WH, Huang YP, Tao X, Zhao JC, Xu YM. Oxidative degradation of organic pollutants utilizing molecular oxygen and visible light over a supported catalyst of $Fe(bpy)_3^{2+}$ in water. *Appl Catal B: Environ*, 2004, 48: 17–24
18 Rosenthal J, Tuckett TD, Hodgkiss JM, Nocera DG. Photocatalytic oxidation of hydrocarbons by a bis-iron(iii)-μ-oxo pacman porphyrin using O_2 and visible light. *J Am Chem Soc*, 2006, 128: 6546–6547
19 Meng X, Qin C, Wang XL, Su ZM, Li B, Yang QH. Chiral salen-metal derivatives of polyoxometalates with asymmetric catalytic and photocatalytic activities. *Dalton Trans*, 2011, 40: 9964–9966
20 Drozd D, Szczubiałka K, Łapok Ł, Sklba M, Patel H, Gorun SM, Nowakowska M. Visible light induced photosensitized degradation of Acid Orange 7 in the suspension of bentonite intercalated with perfluoroalkyl perfluoro phthalocyanine zinc complex. *Appl Catal B: Environ*, 2012, 125: 35–40
21 Kim W, Park J, Jo HJ, Kim HJ, Choi W. Visible light photocatalysts based on homogeneous and heterogenized tin porphyrins. *J Phys Chem C*, 2008, 112: 491–499
22 Ardo S, Achey D, Morris AJ, Abrahamsson M, Meyer GJ. Non-nernstian two-electron transfer photocatalysis at metalloporphyrin-TiO_2 interfaces. *J Am Chem Soc*, 2011, 133: 16572–16580
23 Yella A, Lee HW, Tsao HN, Yi C, Chandiran AK, Nazeeruddin MK, Diau EWG, Yeh CY, Zakeeruddin SM, Gratzel M. Porphyrin-sensitized solar cells with cobalt (II/III)-based redox electrolyte exceed 12 percent efficiency. *Science*, 2011, 334: 629–634
24 Chen X, Ma WH, Li J, Wang ZH, Chen CC, Ji HW, Zhao JC. Photocatalytic oxidation of organic pollutants catalyzed by an iron complex at biocompatible pH values: Using O_2 as main oxidant in a Fenton-like reaction. *J Phys Chem C*, 2011, 115: 4089–4095
25 Ghosh A, Mitchell DA, Chanda A, Ryabov AD, Popescu DL, Upham EC, Collins GJ, Collins TJ. Catalase-peroxidase activity of iron(III)-TAML activators of hydrogen peroxide. *J Am Chem Soc*, 2008, 130: 15116–15126
26 Chung LW, Li X, Hirao H, Morokuma K. Comparative reactivity of ferric-superoxo and ferryl-oxo species in heme and non-heme complexes. *J Am Chem Soc*, 2011, 133: 20076–20079
27 Yamada S. Advancement in stereochemical aspects of Schiff base metal complexes. *Coord Chem Rev*, 1999, 190: 537–555
28 Ruck RT, Jacobsen EN. Asymmetric catalysis of hetero-ene reactions with tridentate schiff base chromium(III) complexes. *J Am Chem Soc*, 2002, 124: 2882–2883
29 Gupta KC, Sutar AK. Catalytic activities of Schiff base transition metal complexes. *Coord Chem Rev*, 2008, 252: 1420–1450
30 Liu L, Jiang DL, Mcdonald A, Hao YQ, Millhauser GL, Zhou FM. Copper redox cycling in the prion protein depends critically on binding mode. *J Am Chem Soc*, 2011, 133: 12229–12237
31 Mohamed RM, Mohamed MM. Copper (II) phthalocyanines immobilized on alumina and encapsulated inside zeolite-X and their applications in photocatalytic degradation of cyanide: A comparative study. *Appl Catal A: Gen*, 2008, 340: 16–24
32 Islam SM, Roy AS, Mondal P, Mubarak M, Mondal S, Hossain D, Banerjee S, Santra SC. Synthesis, catalytic oxidation and antimicrobial activity of copper(II) Schiff base complex. *J Mol Catal A: Chem*, 2011, 336: 106–114
33 Sedai B, Díaz-Urrutia C, Baker RT, Wu RL, "Pete" Silks LA, Hanson SK. Comparison of copper and vanadium homogeneous catalysts for aerobic oxidation of lignin models. *ACS Catal*, 2011, 1: 794–804
34 Ramalingam B, Lee GH, Chen C. Copper complex of aminoisoborneol Schiff base $Cu_2(SBAIB\text{-}d)_2$: An efficient catalyst for direct catalytic asymmetric nitroaldol (Henry) reaction. *Adv Synth Catal*, 2012, 354: 2511–2520
35 Zhang ZJ, Li X, Wang CG, Zhang CC, Liu P, Fang TT, Xiong Y, Xu WJ. A novel dinuclear Schiff-base copper(II) complex modified electrode for ascorbic acid catalytic oxidation and determination. *Dalton Trans*, 2012, 41: 1252–1258
36 Cao TT, Zou CQ, Li RP, Huang YP. Heterogenous degradation of toxic organic pollutants by hydrophobic iron(Ó) Schiff base complex under visible irradiation. *Chem J Chinese Univ*, 2011, 1: 105–112
37 Golcu A, Tumer M, Demirelli H, Wheatley RA. Cd(II) and Cu(II) complexes of polydentate Schiff base ligands: Synthesis, characterization, properties and biological activity. *Inorg Chem Acta*, 2005, 358: 1785–1797
38 Ma JH, Ma WH, Song WJ, Chen CC, Tang YL, Zhao JC, Huang YP, Xu YM, Zang L. Fenton degradation of organic pollutants in the presence of low-molecular-weight organic acids: Co-operative effect of quinone and visible light. *Environ Sci Technol*, 2006, 40: 618–624